GEOPHYSICAL RESEARCH LETTERS, VOL. 20, NO. 11, PAGES 1055-1058, JUNE 7, 1993

SPATIAL CORRELATIONS OF INTERDECADAL VARIATION IN GLOBAL SURFACE TEMPERATURES

Michael E. Mann and Jeffrey Park

Center for the Study of Global Change, Dept of Geology & Geophysics, Yale University

Abstract. We have analyzed spatial correlation patterns of interdecadal global surface temperature variability from an empirical perspective. Using multi-taper coherence estimates from 140-yr records, we find that correlations between hemispheres are significant at $\gtrsim$95% confidence for non-randomness for most of the frequency band $0.06 < f < 0.24$ cyc/yr. Coherence estimates of pairs of 100-yr grid-point temperature data series near 5-yr period reveal teleconnection patterns consistent with known patterns of ENSO variability. Significant correlated variability is observed near 15 year period, with the dominant teleconnection pattern largely confined to the Northern Hemisphere. Peak-to-peak $\Delta T \approx 0.5°$, with simultaneous warming and cooling of discrete patches on the earth's surface. A global average of this pattern would largely cancel.

Introduction

Understanding the nature of interdecadal climate variability has become increasingly important as we seek to separate possible anthropogenic effects from the natural variability of the climate. While it is well established that the climate system exhibits significant internal variability on interannual time scales due to the effects of the quasi-biennial oscillation and ENSO [eg. Peixoto and Oort, 1992; Philander, 1990], there is mounting evidence that the coupled ocean-atmosphere system exhibits significant internal variability on decadal and interdecadal time scales as well [Bjerknes, 1964, Folland et al., 1984, Levitus, 1989, Houghton and Tourre, 1992, Trenberth, 1990]. Recently, Ghil and Vautard [1991], Elsner and Tsonis [1991] and Allen et al. [1992] have analyzed the $\sim$ 140 year instrumental record of global average temperature anomalies of the East Anglia group [Jones et al., 1986abc] for global signals in the decadal and interdecadal ranges. Correlations have been sought with interdecadal oscillations in external astronomical forcing [Loutre et al, 1992]. Using multi-taper spectral analysis [Thomson, 1982; Park et al 1987] on this record, we find no spectral peaks at decadal or longer periods which pass the F-test for phase coherence at 95% confidence levels in both hemispheres. This suggests that, if global climate signals exist at decadal and interdecadal periods, they represent quasiperiodic or aperiodic modes of variability of the climate.

Previous analyses of the global temperature record at interdecadal time scales have focussed on globally or hemispherically averaged temperature series, with little discussion of the spatial correlation patterns or "teleconnections" that should characterize "global" signals. We here examine the correlation patterns, in both amplitude and phase, for spectral variance within narrow frequency band passes. Our approach is empirical, testing the data against the null hypothesis of random spatially uncorrelated temperature signals. An alternative focus would be a statistical test of data prediction from a coupled ocean-atmosphere model. However, such models are not yet reliable enough to preclude our empirical approach. Rather, the data should suggest the phenomena that numerical climate models might be expected to reproduce.

Paper number 93GL00752
0094-8534/93/93GL-00752$03.00

Hemispheric correlations

If global interdecadal temperature oscillations exist in a narrow frequency interval centered on f, we expect the squared coherency $|C(f)|^2$ to be large between temperature time series corresponding to nonoverlapping areas of the Earth's surface. Under the assumption that the values of the discrete Fourier transform are normally distributed in the complex plane with zero mean, statistical tests for nonrandomness, similar to the F variance-ratio test, are described in many texts [Brillinger, 1981; Priestley, 1981]. We use the complex multitaper spectral coherence [Vernon et al 1991], valid for locally white spectral processes

$$C(f) = \frac{\sum_k Y_k^{(1)*}(f) Y_k^{(2)}(f)}{(\sum_k Y_k^{(1)*}(f) Y_k^{(1)}(f) \sum_j Y_j^{(2)*}(f) Y_j^{(2)}(f))^{1/2}} \quad (1)$$

to analyze the coherence between eigenspectral estimates $Y_k^{(1)}(f)$ of series $\{x_n^{(1)}\}_{n=1}^N$ and $Y_k^{(2)}(f)$ of $\{x_n^{(2)}\}_{n=1}^N$. The sums extend over the number of tapers used. A single eigenspectral estimate is defined by

$$Y_k(f) = \sum_{n=1}^{N} \nu_n^{(k)} x_n e^{i2\pi f n \Delta t} \quad (2)$$

where Δt is the sampling interval. The Slepian data taper $\{\nu_n^{(k)}\}_{n=1}^N$ is the kth member of an orthogonal set of tapers, determined by a variational condition to minimize spectral leakage outside a chosen central bandwidth. In our analysis, six 4π-prolate tapers were chosen as a compromise between spectral resolution and variance. A parallel analysis using five 3π-prolate tapers yielded no significant differences.

Figure 1 shows the correlation between the annually-averaged $\sim$ 140-year combined land and sea surface temperature anomaly records for the southern and northern hemispheres [Jones et al., 1986c] and their respective power spectra at periods greater than 4 yr (at shorter periods, the aliasing bias of the annually-averaged data is signifi-

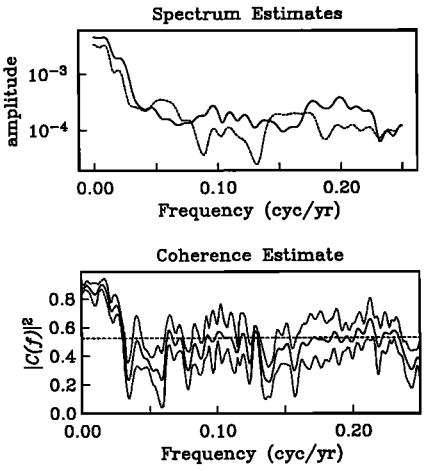

Fig. 1. Upper: multitaper spectrum estimates for combined land-sea annual average temperature anomalies for the northern (solid) and southern (dashed) hemispheres. The spectra are locally white except at very low frequency. Lower: multitaper squared coherence estimate $|C(f)|^2$ between the two records. The associated $1 - \sigma$ jackknife uncertainties are indicated by dashed lines. Note that $|C(f)|^2 \gtrsim 0.5$ (95% confidence) occurs in a relatively narrow band near 15 year period, as well as near 10 and 5 year periods.

cant). Fluctuations in $|C(f)|^2$ with scale length near the Rayleigh frequency f_R (roughly 0.007 cycle/year for a 140-year data series) should be ignored. The 4π-prolate tapers average over a central half-bandwidth of $4f_R$, or approximately 0.03 cycle/year. Correlations are extremely high (99% confidence for non-randomness) near zero frequency (40 yr period and greater) representing the recent secular warming trend. While not globally uniform, this trend shows clear global-scale correlations [Hansen and Lebedeff, 1987] and is the dominant signal in the observational record of global temperature [Kuo et al 1990, Ghil and Vautard, 1991]. For $0.06 < f < 0.24$ cyc/yr (between 4 and 16 yr period), $0.4 \lesssim |C(f)|^2 < 0.6$, the bounds corresponding to 92% and 99% confidence for nonrandomness, respectively. For comparison, the median (50% confidence) of the statistical distribution occurs at $|C(f)|^2 \approx 0.13$. The peak at $f = 0.04$ cyc/yr (25 years) occurs in the frequency range where the spectral amplitudes vary abruptly, and the locally white assumption of the eigenspectral estimates $Y_k(f)$ is suspect. The large jackknife error bounds on $|C(f)|^2$ here indicate the doubt regarding the significance of this peak.

The bias in $C(f)$ caused by the incomplete coverage of the historical record is unknown, and cannot be discounted. Nevertheless, the correlation between the hemispherically averaged series at interdecadal periods appears significant, though far less compelling than for the secular trend. Further insight requires a more detailed examination of the associated spatial correlation patterns.

Spatial correlation patterns

We examined the coherence of 100 year monthly temperature records of individual 5° by 5° land and sea surface temperature grid-points [P. Jones, from NCAR, unpublished] in band passes centered at 5 and 15 yr period. Five year period corresponds roughly to the center of the ENSO frequency band. As shown in Figure 1, 15 year period is the longest period, above the secular trend, for which $|C(f)|^2$ breaches the 95% confidence level for nonrandomness. $|C(f)|^2$ at $f = 1/15$ yr^{-1} averages interdecadal spectral information between roughly 10 and 33 year periods. We choose 1890 as a lower cutoff date for the grid-point data series. Allowing only small gaps in the monthly data, we obtain 449 grid points with nearly continuous 100 year long coverage. The number of statistically independent data series is limited by strong correlations between neighboring grid points. Such short range correlations have a frequency-independent signature. For example, while a group of neighboring grid points in central Asia is correlated at all bandpasses, spatial correlation patterns corresponding to 3–7 year ENSO variability [see eg., Peixoto and Oort, 1992] are observed only in the appropriate bandpass. We estimated the short-range correlation length to be roughly 1500 km from pairwise gridpoint correlations. This reduces the effective spatial degrees of freedom from 449 to about 40. Background noise may give rise to spurious correlations. For example, a collection of uncorrelated data series would give rise to 5 spurious correlations at 95% confidence for every 100 cases. However, random values of $C(f)$ should have random complex phase, and scatter about a circle in the complex plane.

The teleconnection patterns of ENSO are fairly well established (e.g. Philander, 1990). For 100 year time series, 4π-prolate tapers will average spectral variance over a bandpass with halfwidth $\Delta f = 0.04$ cyc/year. A coherence estimate at 5-yr period (0.2 cyc/yr) averages signals in the 4–6 year range, capturing much of the characteristic ENSO variability. Figure 2 shows all grid points, correlated with a reference grid point near Darwin, Australia, superimposed on an idealized map of precipitation anomalies associated with typical ENSO episodes (after Ropelewski and Halpert [1987]). The observed temperature pattern agrees well with the ENSO precipitation anomaly pattern where grid point data is available. Figure 3 shows the corresponding correlation phase relationships, where points are numbered according to the phase progression of the precipitation anomalies. Aside from the two outlying points in

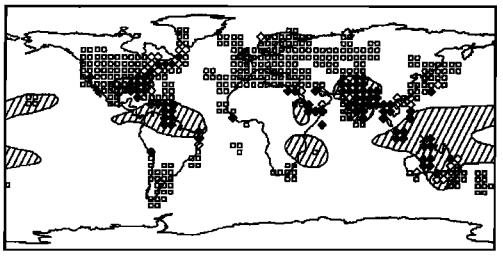

Fig. 2. Temperature teleconnections near 5 year period corresponding to ENSO related variability. Grid points shown as filled diamonds correlate at > 95% confidence levels with the reference point near Darwin, Australia. Unfilled diamonds correlate at > 90% confidence levels, and all other points correlate below 90% confidence (usually much lower). The pattern is consistent with known ENSO precipitation teleconnections, indicated by shaded regions.

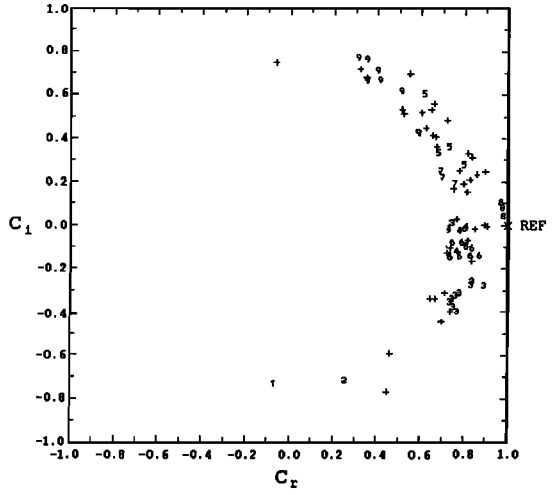

Fig. 3. Phase relationships of teleconnection pattern shown in Fig. 1. Complex spectral coherence is plotted, restricted to values above 95% confidence. Points are numbered in the order in which precipitation anomalies are first observed in those areas. "1" = western US, "2" = southern coastal Australia, "3" = northern India, "4" = central Australia, "5" = the far western Pacific, "6" = the Caribbean and northern South America, "7" = southern India, "8" = northern Australia, "9" = the southeastern US. and a "+" = other grid points. The phase of the temperature correlations is roughly consistent with precipitation in both order and timing. For instance, the temperature signal first appears in north India, later in the southeastern US. The correlation phase extends over roughly 100° (~1.5 year) between those two regions.

southern Australia and western US, the phase relations are in good agreement, with ~7 month lag between northern India and the southeastern US. This correlated variability contributes to the significant correlations we observe between the two hemispheres near 5 year period, and to the significant spectral power attributed to ENSO in the global average temperature record [Jones, 1989; Angell, 1990].

We observe statistically significant teleconnection patterns in the 15 year bandpass. Figure 4 shows the dominant pattern, with correlated variability confined largely to the Northern Hemisphere, including portions of the eastern and western United States, the Caribbean, Northern Europe, Levant, India and central Europe. A reference grid point in the Pacific Northwest is chosen, but the observed pattern is largely robust with respect to choice of reference. Figure 5 shows the correlation phase relationship associated with this teleconnection pattern. The reference point is correlated near zero phase (positive correlation) with gridpoints in the western US, the Caribbean, India, Levant, and central Europe. The phases scatter roughly 30°, corresponding to temporal lags of roughly a year. Points in the eastern US and northern Europe are nearly 180° degrees out of phase (ie, negatively correlated) with the rest of the observed pattern. Such teleconnections may have their origins in the interaction between sea-surface temperature variability, surface pressure anomalies, and associated changes in the planetary wave structure. Negative correlation between grid-points in the the western US and Hawaii, and the southeastern US is consistent with Trenberth [1990], which examined changes in the Pacific-North American (PNA) teleconnection on interdecadal time scales, albeit with a much shorter time series. Our analysis suggests a more widely correlated pattern of variability. The correlation phases indicate simultaneous warming and cooling of different surface regions in the Northern Hemisphere with a time scale near 15 years. Unlike the ENSO temperature variations, which are largely positively correlated, a global average of this pattern would largely cancel. The majority of grid points in the above teleconnection pattern exhibit peak to peak fluctuations $\gtrsim 0.5°$ in amplitude. Using globally averaged data, Ghil and Vautard [1991] argued for bidecadal temperature oscillations with peak to peak amplitude of only 0.2°.

Teleconnections of temperature anomalies in the 15 year bandpass are also observed in the Southern Hemisphere, chiefly involving coastal areas bordering on the Antarctic Circumpolar Current, as well as parts of India and southern Asia. This correlation pattern is less robust with respect to the choice of reference point, and the correlation

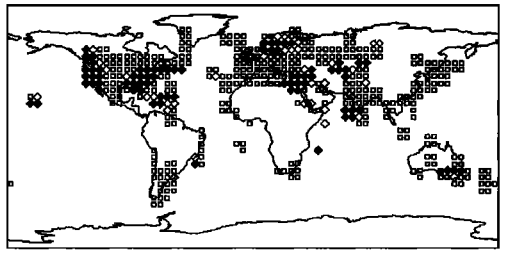

Fig. 4. Northern hemisphere teleconnection pattern in the 15 year bandpass. Large scale teleconnections are clearly evident, reaching from the western US to southern India and parts of central Asia. A reference point in northwestern US is chosen, but the teleconnection pattern is robust with respect to reference point in the correlation pattern.

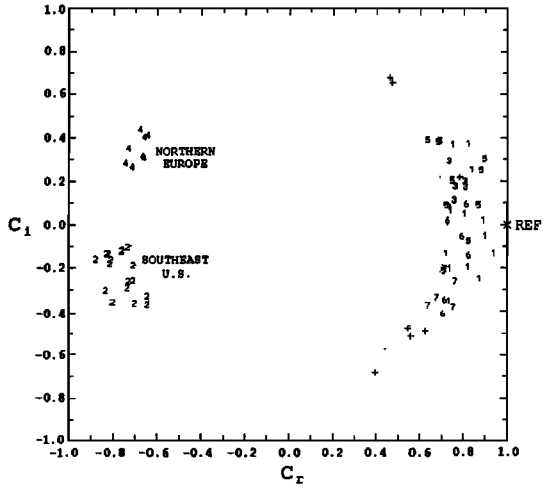

Fig. 5. Correlation phases associated with the teleconnection pattern shown in Fig. 4. "1"= western US., "2" = eastern US., "3"= Caribbean, "4"= northern Europe, "5"= the Levant, "6"= central Europe, and "7" = southern India. Note that the eastern US and northern Europe are roughly 180° out of phase with the rest of the pattern.

phases do not show a clear geographical relationship. The correlations between the two hemisphere averaged records probably arise from an overlap between these correlations and the ones shown above.

Conclusions

Spatial correlations in historical temperature measurements confirm the global nature of the secular warming trend and low frequency ENSO variability. Statistically significant teleconnections of temperature anomalies at interdecadal periods are also observed. The associated correlation patterns appear less widespread than those of ENSO or of the secular trend, and an examination of other climate indexes would be required to confirm them as constituting a true "global" climatic signal.

Our analysis argues for a careful examination of the spatial dependence of any putative long-period global climatic signal. Internal climate oscillations are expected to redistribute heat over the earth's surface, as well as between the atmosphere and ocean. Predictions of climate change based on the analysis of globally averaged data may be valid only in certain regions of the globe, or, worse, may be a deceptive average of two or more independent regional climate processes. Temperature records for all 449 land grid points in our analysis exhibit variability in the 15-year bandpass, but spatial correlations are significant for only a subset of the gridpoints and may be due to combinations of at least two independent processes. ENSO variation in surface temperature is largely positively correlated over the globe, but interdecadal variability is not.

Acknowledgments. We wish to thank Dr. Tom Boden of CDIAC and Dr. Roy Jenne of NCAR for information regarding various temperature data sets used. M. Mann has been supported by NASA grant NAG8-785 and EPRI grant RP 2333-11. J. Park has been supported by NSF grant EAR-8657206.

References

Allen, M. R., Read, P. L., and Smith, L.A., Temperature time series, *Nature*, *355*, 686, 1992.

Angell, J.K., Variation in global tropospheric temperature after adjustment for the El Nino influence, 1958-1989, *Geophys. Res. Lett.*, *17*, 1093–1096, 1990.

Berger, A., Melice, J. L., and Hinnov, L., A strategy for frequency spectra of Quaternary climate records, *Climate Dynamics*, *5*, 227–240, 1991.

Bjerknes, J., Atlantic air-sea interactions, *Adv. Geophys.*, *10*, 1–82, 1964.

Brillinger, D. R., *Time Series, Data Analysis and Theory*, Holden-Day, San Francisco, 1981.

Elsner, J. B. and Tsonis, A. A., Do bidecadal oscillations exist in the global temperature record?, *Nature*, *353*, 551–553, 1991.

Folland, C. K., Parker, D. E., and Kates, F. E., Worldwide marine temperature fluctuations 1856-1981, *Nature*, *310*, 670–673, 1984.

Ghil, M., and Vautard, R., Interdecadal oscillations and the warming trend in global temperature time series, *Nature*, *350*, 324–327, 1991.

Hansen, J., and Lebedeff, S., Global trends of measured surface air temperature, *J. Geophys. Res.*, *92*, 13345–13372, 1987.

Houghton, R., and Tourre, Y., Characteristics of low-frequency sea-surface temperature fluctuations in the tropical Atlantic, *Journal of Climate 5*, 765–771, 1992.

Jones, P.D., The influence of ENSO on global temperatures, *Climate Monitor*, *17*, 80-89, 1989.

Jones, P. D., Raper, S. C., Bradley, R. S., Diaz, H. F., Kelly P. M., and Wigley, T.M., Northern hemisphere surface air temperature variations, *J. Clim. appl. Met.*, *25*, 161–179, 1986.

Jones, P. D., Raper, S. C., and Wigley, T. M., Southern hemisphere surface air temperature variations, *J. Clim. appl. Met.*, *25*, 1213–1230, 1986.

Jones, P. D., Wigley, T. M., and Wright, P. B., Global temperature variations between 1861 and 1984, *Nature*, *322*, 430–434, 1986.

Kuo, C., Lindberg, C. and Thomson, D. J., Coherence established between atmospheric carbon dioxide and global temperature, *Nature*, *343*, 709–713, 1990.

Levitus, S., Interpentadel variability of temperature and salinity at intermediate depths of the North Atlantic ocean, 1970-1974 vs 1955-1959, *J. Geophys. Res.*, *94*, 6091–6131, 1989.

Park, J., C. R. Lindberg, and Vernon, F. L. III, Multitaper spectral analysis of high-frequency seismograms, *J. Geophys. Res.*, *92*, 12675–12684, 1987.

Loutre, M. F., Berger, A., Bretagnon, P., and Blanc, P. L., Astronomical frequency for climate research at the decadal to century time scale, *Climate Dynamics*, *7*, 1992.

Peixoto, J. P., and Oort, A. H., *Physics of Climate* , American Institute of Physics, New York, 1992.

Philander, S. G., *El Nino, La Nina, and the Southern Oscillation*, Academic Press, San Diego, 1990.

Priestley, M. B., *Spectral Analysis and Time Series*, Academic Press, San Diego, 1981.

Ropelewski, C. F., and Halpert, M. S., Global and regional scale precipitation patterns associated with the El Nino/Southern Oscillation, *Mon. Weath. Rev.*, *115*, 1606–1626, 1987.

Thomson, D. J., Spectrum estimation and harmonic analysis, *IEEE Proc.*, *70*, 1055–1096, 1982.

Trenberth, K. E., Recent observed interdecadal climate changes in the Northern Hemisphere, *Bull. Am. Met. Soc.*, *71*, 988–993, 1990.

Vernon, F. L., Fletcher, J., Carroll, L., Chave, A., and Sembrera, E., Coherence of seismic body waves from local events as measured by a small-aperture array, *J. Geophys. Res.*, *96*, 11981–11996, 1991.

M. E. Mann and J. Park, Department of Geology and Geophysics P.O. Box 6666, Yale University, New Haven, CT 06511

(Received: December 23, 1992;
Accepted: March 23, 1993)